Corrosion and strength degradation of Si_3N_4 and sialons in K_2CO_3 and K_2SO_4 melts

T. SATO, Y. KOIKE, T. ENDO, M. SHIMADA
Department of Applied Chemistry, Faculty of Engineering, Tohoku University, Sendai 980, Japan

Si_3N_4-based ceramics, such as hot isostatically pressed Si_3N_4, hot-pressed Si_3N_4, hot-pressed sialons containing 0, 30, 60 and 100% α phase, were corroded by K_2SO_4 and K_2CO_3 melts at 1150 to 1300 and 925 to 1150° C, respectively. The surface chemical reaction-controlled shrinking core model adequately described the relationship between the weight loss of the specimen and time for the corrosion reactions in both K_2SO_4 and K_2CO_3 melts, and the apparent activation energies were 380 to 608 and 157 to 344 kJ mol^{-1}, respectively. The corrosion rate in K_2CO_3 melt decreased with increasing content of aluminium and yttrium ions in the specimens, but no systematic relation was observed for the reaction in K_2SO_4 melts. The fracture strength of the specimens corroded by K_2SO_4 and K_2CO_3 melts degraded to 2/3 to 2/5 of the original values up to a 2% weight loss, and then was almost constant up to 30% weight loss.

1. Introduction

Non-oxide ceramics such as Si_3N_4 and SiC show excellent physical properties, such as high-temperature fracture strength/fracture toughness and thermal shock resistance. However, these ceramics are inherently unstable in an oxidizing atmosphere. It is essential to investigate the effect of hot corrosion attack on the mechanical properties in these non-oxide ceramics for high-temperature structural applications, such as heat exchangers, hot gas turbines and magnetohydrodynamic (MHD) generators. Mayer and Riley [1], Erdoes and Altorfer [2], Tressler *et al.* [3], Bourne and Tressler [4], Ferber and Tennery [5], Becher [6] and Sato *et al.* [7] have investigated the corrosion behaviour of Si_3N_4 ceramics in a variety of molten salt/gas environments, and reported that the corrosion behaviour was dependent on the chemical environments. Tressler *et al.* [3] reported that the degree of corrosion of Si_3N_4 depended on the free O^{2-} ions in the molten salts. Borne and Tressler [4] reported that exposures of hot-pressed Si_3N_4 and reaction-bonded Si_3N_4 to deep melts of NaCl or NaCl + Na_2SO_4 resulted in strength degradation of 30 to 60%, both at room temperature and at 800 to 1200° C. The decrease in strength was due to a significant increase in the critical flaw size. Becher [6] reported that the degradation of the fracture strength of Si_3N_4 exposed to coal slags at high temperature, depended on the chemical constitution of the slags, i.e. fracture strength of hot-pressed Si_3N_4 exposed in an acid slag decreased up to 65%, but a basic slag caused remarkably little strength degradation in spite of the large corrosion rate. In general, it was considered that oxide additives such as MgO, Y_2O_3 and Al_2O_3 in the ceramics contributed to preferential attack via a complex liquid silicate formation [8], but no systematic study for the effect of additives on the corrosion behaviour has yet been reported. In a previous study [7], we reported the stoichiometry and kinetics of the corrosion reaction of sintered Si_3N_4 in various alkali sulphate and alkali carbonate melts. The aims of the present study are to report the effect of the additives on the corrosion rate and strength degradation in K_2SO_4 and K_2CO_3 melts.

2. Experimental procedure

Hot isostatically pressed Si_3N_4 without additives, hot-pressed Si_3N_4 and hot-pressed sialons containing 0, 30, 60 and 100% α phase, denoted HIP-Si_3N_4, HP-Si_3N_4, SiAlON-0, SiAlON-30, SiAlON-60 and SiAlON-100, were used as corrosion samples. The characteristics of these ceramics are summarized in Table I. HIP-Si_3N_4, HP-Si_3N_4 and SiAlON-0 were

TABLE I Characteristics of the samples

Sample	Phase	Chemical compositions (at. %)					K_{IC} (MPa m$^{1/2}$)	σ_{3b} (MPa)
		Si	N	Y	Al	O		
HIP-Si_3N_4	β	42.9	57.1	0	0	0	3.98	753
HP-Si_3N_4	β	41.2	54.8	0.86	0.76	2.44	5.29	870
SiAlON-0	β	38.5	52.4	0.86	3.51	4.77	3.60	935
SiAlON-30	$\alpha + \beta$	41.2	56.4	0.34	1.58	0.51	4.31	717
SiAlON-60	$\alpha + \beta$	37.6	55.0	1.06	4.77	1.59	5.01	702
SiAlON-100	α	34.2	53.5	1.74	7.94	2.65	4.94	552

α, α-Si_3N_4 phase; β, β-Si_3N_4 phase.

0022–2461/88 $03.00 + .12

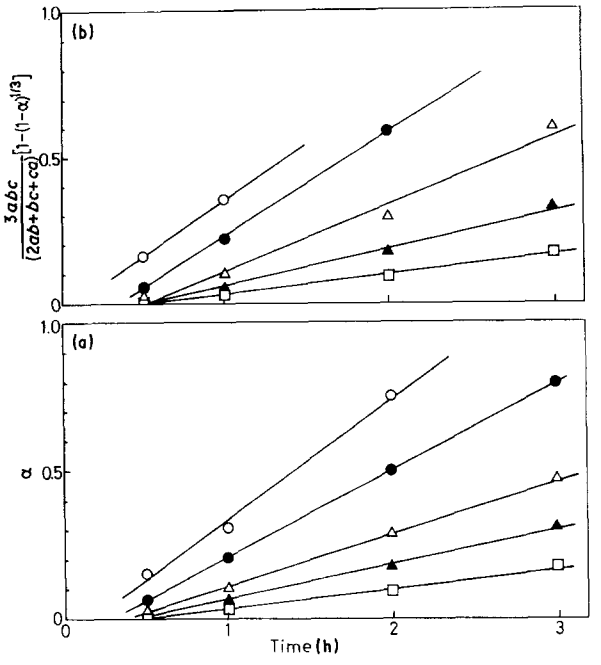

Figure 1 Time dependence of weight loss for HP-Si_3N_4 specimens in K_2SO_4 melts exposed to nitrogen gas at various temperatures. (○) 1300° C, (●) 1275° C, (△) 1250° C, (▲) 1225° C, (□) 1200° C.

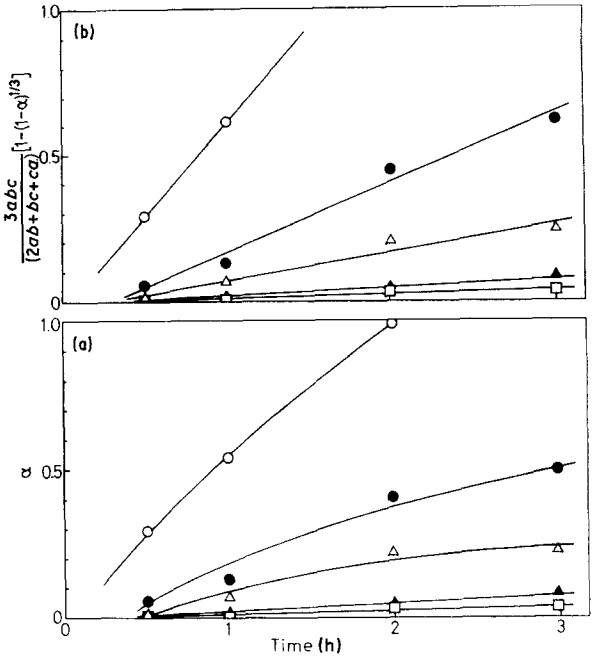

Figure 2 Time dependence of weight loss for HP-Si_3N_4 specimens in K_2CO_3 melts exposed to nitrogen gas at various temperatures. (○) 1150° C, (●) 1100° C, (△) 1050° C, (▲) 1000° C, (□) 975° C.

β-Si_3N_4 phase and SiAlON-100 was α-Si_3N_4 phase. On the other hand, SiAlON-30 and SiAlON-60 were mixtures of α-Si_3N_4 and β-Si_3N_4 phase. The amounts of α-Si_3N_4 phase determined by Gazzara and Meissier's method [9] were 30 and 60%, respectively.

A diagram of the experimental apparatus has already been given in our previous paper [10]. All samples were cut into rectangular coupons, 4 mm by 5 mm by 15 mm. In each experiment, a weighed sample and powdered reagent-grade K_2SO_4 and K_2CO_3 were put into a test tube of highly purified alumina, 16 mm in diameter and 105 mm long, then placed in an electric furnace regulated at the desired temperature. The amounts of K_2SO_4 and K_2CO_3 added were five times that of the stoichiometry, based on Equations 1 and 2.

$$16Si_3N_4 + 27K_2SO_4 = 12(K_2O \cdot 4SiO_2) + 32N_2 + 15K_2S_{1.8} \quad (1)$$

$$24Si_3N_4 + 81K_2CO_3 = 18(K_2O \cdot 4SiO_2) + 48N_2 + 81CO + 126K \quad (2)$$

Nitrogen gas (> 99.99% purity) was injected into the tube at a rate of 20 ml min^{-1} throughout the reaction. After maintaining the desired temperature and time, the tube was removed from the electric furnace and cooled quickly to room temperature. The samples were washed in hot water, dried, and weighed. The crystalline phase and microstructure of the samples were examined by X-ray diffraction analysis (XRD), infrared spectroscopy and scanning electron microscopy (SEM). The fracture strength of the sample was determined by three-point bending test with a cross-head speed of 0.5 mm min^{-1} and span length of 10 mm.

3. Results and discussion

The time dependence of the degree of the weight loss for HP-Si_3N_4 immersed in K_2SO_4 melts at 1200 to 1300° C and K_2CO_3 melts at 975 to 1150° C exposed to nitrogen gas is shown in Figs 1 and 2. A significant weight loss of HP-Si_3N_4 in K_2SO_4 and K_2CO_3 melts was observed above 1200 and 975° C, respectively. In the heterogeneous reaction systems such as solid and liquid phases, when the shrinking core model is applied and the surface chemical process is rate-limiting, the relation between the fractional conversion, α, and time, t, is expressed by Equation 3.

$$1 - (1 - \alpha)^{1/3} = kt/r_0 \quad (3)$$

where r_0 is the radius of the sample and k is the rate constant. As the specimens used in the present study are rectangular coupons, r_0 is defined as $3abc/2(ab + bc + ca)$, where a is the specimen width, b is the specimen thickness and c is the specimen length, respectively. As seen in Figs 1 and 2, the surface chemical reaction-controlled shrinking core model adequately described the relation between time and fractional conversion of HP-Si_3N_4 in both K_2SO_4 and K_2CO_3 melts exposed to nitrogen. Similar experiments were carried out for all specimens and the apparent activation energies and frequency factors in the Arrhenius equation were determined. The results are summarized

TABLE II Frequency factors, A, and apparent activation energies, E, for the oxidation of various Si_3N_4-based ceramics in K_2SO_4 and K_2CO_3 melts

Sample	A (mm h^{-1})		ΔE (kJ mol^{-1})	
	K_2SO_4 corrosion	K_2CO_3 corrosion	K_2SO_4 corrosion	K_2CO_3 corrosion
HIP-Si_3N_4	1.01×10^{15}	3.27×10^{6}	447	157
HP-Si_3N_4	7.66×10^{13}	3.75×10^{11}	424	320
SiAlON-0	1.54×10^{18}	1.25×10^{9}	548	257
SiAlON-30	2.46×10^{12}	8.00×10^{8}	380	250
SiAlON-60	1.60×10^{16}	3.22×10^{12}	493	344
SiAlON-100	4.21×10^{20}	2.85×10^{9}	608	275

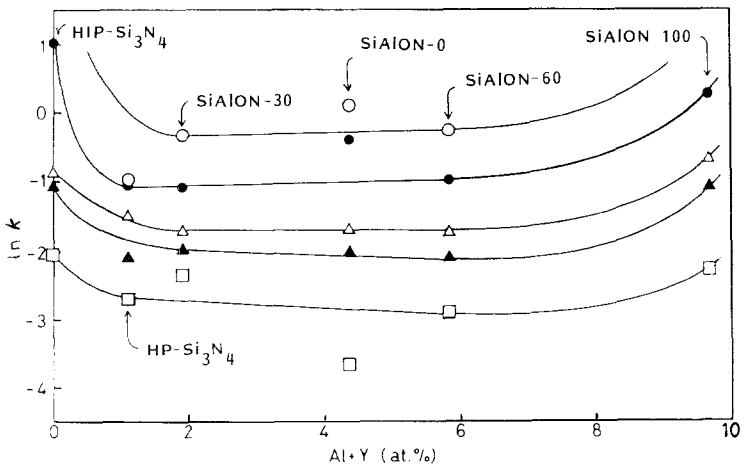

Figure 3 Relationship between the corrosion rate constants and the content of aluminium and yttrium ions for Si_3N_4-based ceramics in K_2SO_4 melts. (○) 1300° C, (●) 1275° C, (△) 1250° C, (▲) 1225° C, (□) 1200° C.

in Table II. The apparent activation energies for the corrosion reaction of Si_3N_4 and sialons were 380 to 608 kJ mol^{-1} in K_2SO_4 melts and 157 to 344 kJ mol^{-1} in K_2CO_3. The corrosion rate seemed to depend on the contents of additives. The corrosion rate constant for each Si_3N_4-based ceramic in K_2SO_4 melts and K_2CO_3 melts is plotted against the total content of aluminium and yttrium ions in Figs 3 and 4. In both potassium melts, the corrosion rate of HIP-Si_3N_4 without additives was significantly fast. As seen in Fig. 4, the corrosion rate in K_2CO_3 melts decreased with increasing contents of aluminium and yttrium ions, and the corrosion rate was in the order HIP-Si_3N_4 ≫ HP-Si_3N_4 > SiAlON-30 > SiAlON-0 > SiAlON-60 > SiAlON-100. These results might be due to the protection of the corrosion reaction by Al_2O_3 and Y_2O_3. On the other hand, the corrosion rate in K_2SO_4 melts decreased with increasing content of aluminium and yttrium ions up to 1 at. %. It was almost constant up to 6 at. %, but increased again above 9.7 at. %. The corrosion rate in K_2SO_4 melts was in the order of HIP-Si_3N_4 > SiAlON-100 > SiAlON-60 ≃ SiAlON-0 ≃ SiAlON-30 ≃ HP-Si_3N_4. By X-ray powder diffraction analysis on the surface of the specimens corroded in both K_2SO_4 and K_2CO_3 melts, no diffraction peak corresponding to a corrosion product was detected. On the other hand, as shown in Fig. 5, the adsorption peak at 1100 cm^{-1} corresponding to Si–O stretching was observed in the infrared spectrum of the specimen corroded in the K_2SO_4 melt, but was not observed in the sample corroded in the K_2CO_3 melt. These results indicated that amorphous silica was formed on the surface of the specimen corroded by the K_2SO_4 melt, and it played a significant role in the corrosion reaction. It was reported that the crystallization of amorphous silica formed on the surface of Si_3N_4 by oxidation at high temperature was greatly enhanced by MgO and/or Y_2O_3 doped in the specimen. Therefore, it was suspected that the crystallization of amorphous silica formed on the specimen containing a large amount of Y_2O_3 in K_2SO_4 melts proceeded rapidly and caused the formation of microcracks; hence the corrosion rate increased at high yttrium ion contents.

The corrosion of Si_3N_4-based ceramics by both K_2SO_4 and K_2CO_3 melts resulted in extensive roughening of the surface of the specimens, which greatly degraded the fracture strength. The fracture strength of the specimens corroded in K_2SO_4 and K_2CO_3 melts was determined by a three-point bending test using Equation 4.

$$\sigma_{3b} = 3PL/2ab^2 \quad (4)$$

where P is the applied load and L is the span length. The dimensions of samples, a and b, were measured on the unpolished corroded specimens. The fracture strengths determined are shown in Figs 6 and 7 as a function of weight loss of the specimens. The bending strength of all specimens corroded in both potassium melts degraded to 2/3 to 2/5 of the original values up

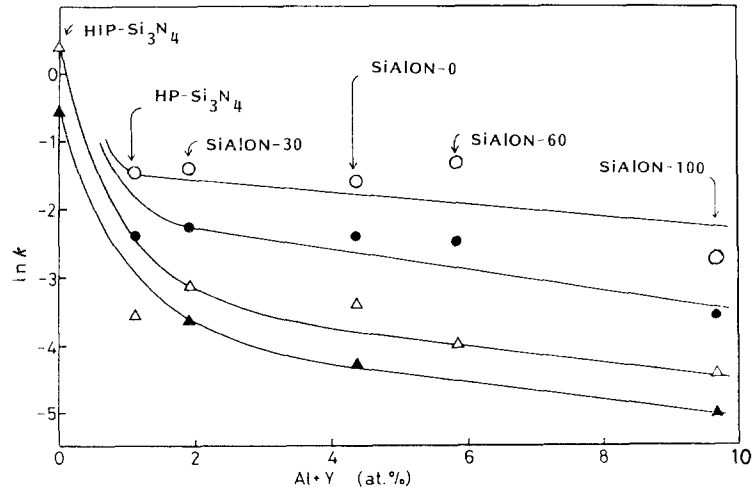

Figure 4 Relationship between the corrosion rate constants and the content of aluminium and yttrium ions for Si_3N_4-based ceramics in K_2SO_4 melts. (○) 1100° C, (●) 1050° C, (△) 1000° C, (▲) 950° C.

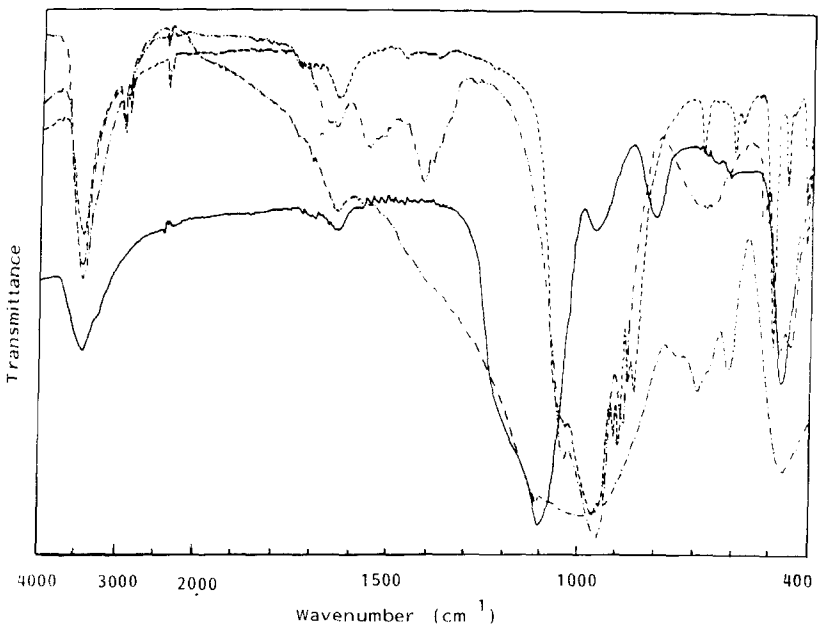

Figure 5 Infrared spectra of HIP-Si_3N_4 corroded in K_2SO_4 melts and K_2CO_3 melts. (——) SiO_2 powder, (– – –) Si_3N_4 powder, (–·–) product in Si_3N_4–K_2SO_4 system, (–··–) product in Si_3N_4–K_2CO_3 system.

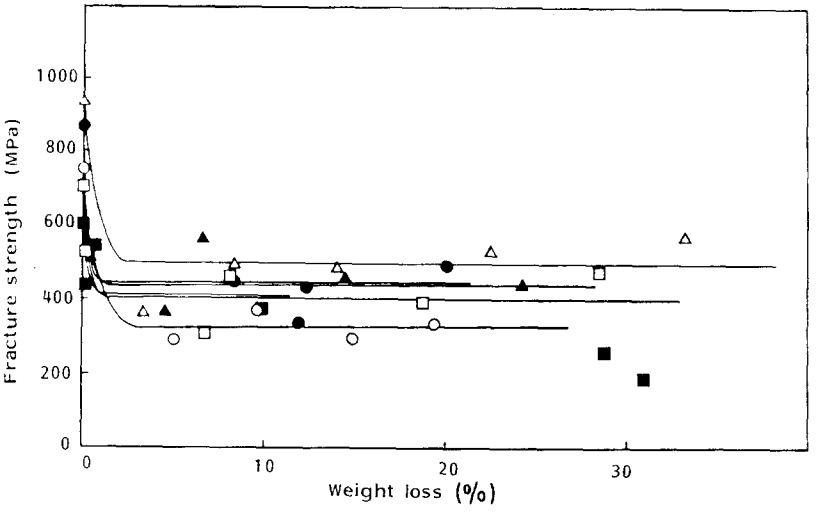

Figure 6 Relationship between the bending strength and the weight loss for Si_3N_4-based ceramics corroded in K_2SO_4 melts. (○) HIP-Si_3N_4, (●) HP-Si_3N_4, (△) SiAlON-0, (▲) SiAlON-30, (□) SiAlON-60, (■) SiAlON-100.

to a 2% weight loss, and then remained almost constant up to a 30% weight loss. These results indicated that the flaws about two to six times larger than the original ones were formed in the initial stage of the corrosion reaction within the 2% weight loss, and then the flaw size remained almost constant during the subsequent corrosion reaction. The flaw size, C, of each Si_3N_4-based ceramic introduced by the corrosion in K_2SO_4 and K_2CO_3 melts was calculated from Equation 5 using

$$C = K_{IC}^2/\pi\sigma_{3b}^2, \quad (5)$$

values of the fracture toughness, K_{IC} and the fracture strength, σ_{3b}, shown in Table I and Figs 6 and 7. The results are given in Table III. Scanning electron micrographs of a cross-section of the SiAlON-100 corroded in K_2SO_4 at 1150° C for 1 to 3 h and in K_2CO_3 at 925° C for 1 to 3 h are shown in Fig. 8. Extensive roughening and the formation of large pits were observed on the surface of the corroded specimens. The corroded layer thickness of the specimens dipped in K_2SO_4 and K_2CO_3 melts was almost constant up to 3 h, and was about 40 and 25 μm, respectively. These results agreed well with those shown in Figs 6 and 7 and Table III.

TABLE III Flaw length in various Si_3N_4-based ceramics corroded in K_2SO_4 melts at 1150° C and K_2CO_3 melts at 925° C

Sample	Before corrosion (μm)	After corrosion (μm)	
		in K_2SO_4	in K_2CO_3
HP-Si_3N_4	8.67	48.0	24.4
HIP-Si_3N_4	11.8	44.0	19.2
SiAlON-0	4.72	16.5	9.76
SiAlON-30	11.5	30.5	21.9
SiAlON-60	16.2	47.5	25.5
SiAlON-100	25.5	44.0	53.5

By assuming isotropic shrinkage of the sample due to the corrosion reaction, Equation 4 can be modified as follows

$$\sigma_{3b} = 3PL/2a_0b_0^2(1-x)^3 = 3PL/a_0b_0^2(1-\alpha) \quad (6)$$

where a_0 and b_0 are the initial width and thickness of the specimen and x is the degree of the shrinkage of the specimen. As it is possible to estimate the flaw size and the degree of corrosion for the specimen immersed in K_2SO_4 and K_2CO_3 melts from the present experimental results, the prediction of time rupture for the corroded specimen might be possible. By using

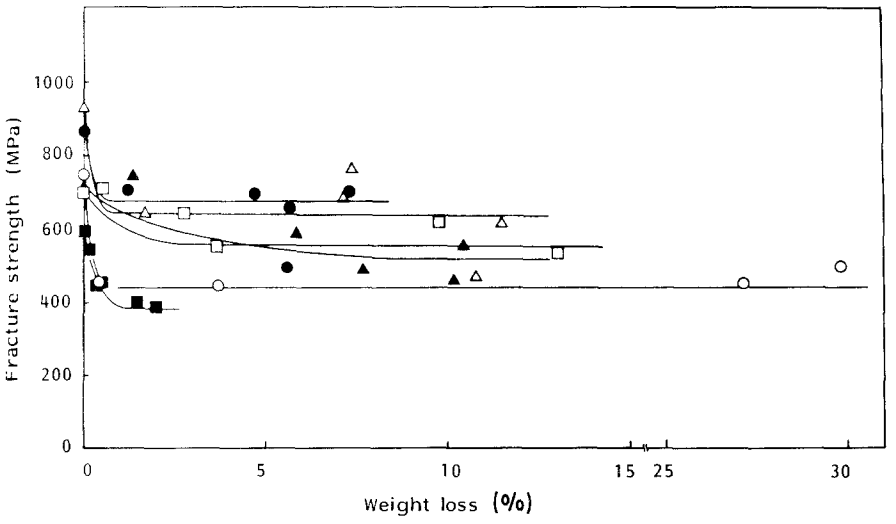

Figure 7 Relationship between the bending strength and the weight loss for Si_3N_4-based ceramics corroded in K_2CO_3 melts. (○) HIP-Si_3N_4, (●) HP-Si_3N_4, (△) SiAlON-0, (▲) SiAlON-30, (□) SiAlON-60, (■) SiAlON-100.

Equations 3, 5 and 6 and the Arrhenius equation of $k = A \exp(-\Delta E/RT)$, where A and E are given in Table II, the predicted time to rupture for the corroded samples at 1100° C under a load of 0.3 P was calculated using the initial sample size of 50 mm × 50 mm × 50 mm, where P corresponds to the fracture load of the uncorroded original sample. The results are listed in Table IV. It should be noted that the resistance to the corrosion of Si_3N_4-based ceramics is greatly increased by adding Al_2O_3 and Y_2O_3, and SiAlON-100 showed the greatest resistance to corrosion in both K_2SO_4 and K_2CO_3 melts at 1100° C.

4. Conclusions

From the present experimental results, the following conclusions may be drawn.

1. The surface chemical reaction-controlled shrinking core model could be applied to describe the relationship between the degree of the corrosion and the reaction time for the corrosion of Si_3N_4-based ceramics in K_2SO_4 and K_2CO_3 melts.

2. The apparent activation energies for the corrosion of Si_3N_4-based ceramics in K_2SO_4 and K_2CO_3 melts were 380 to 608 and 157 to 344 kJ mol^{-1}, respectively.

3. The corrosion rate in K_2CO_3 melts decreased

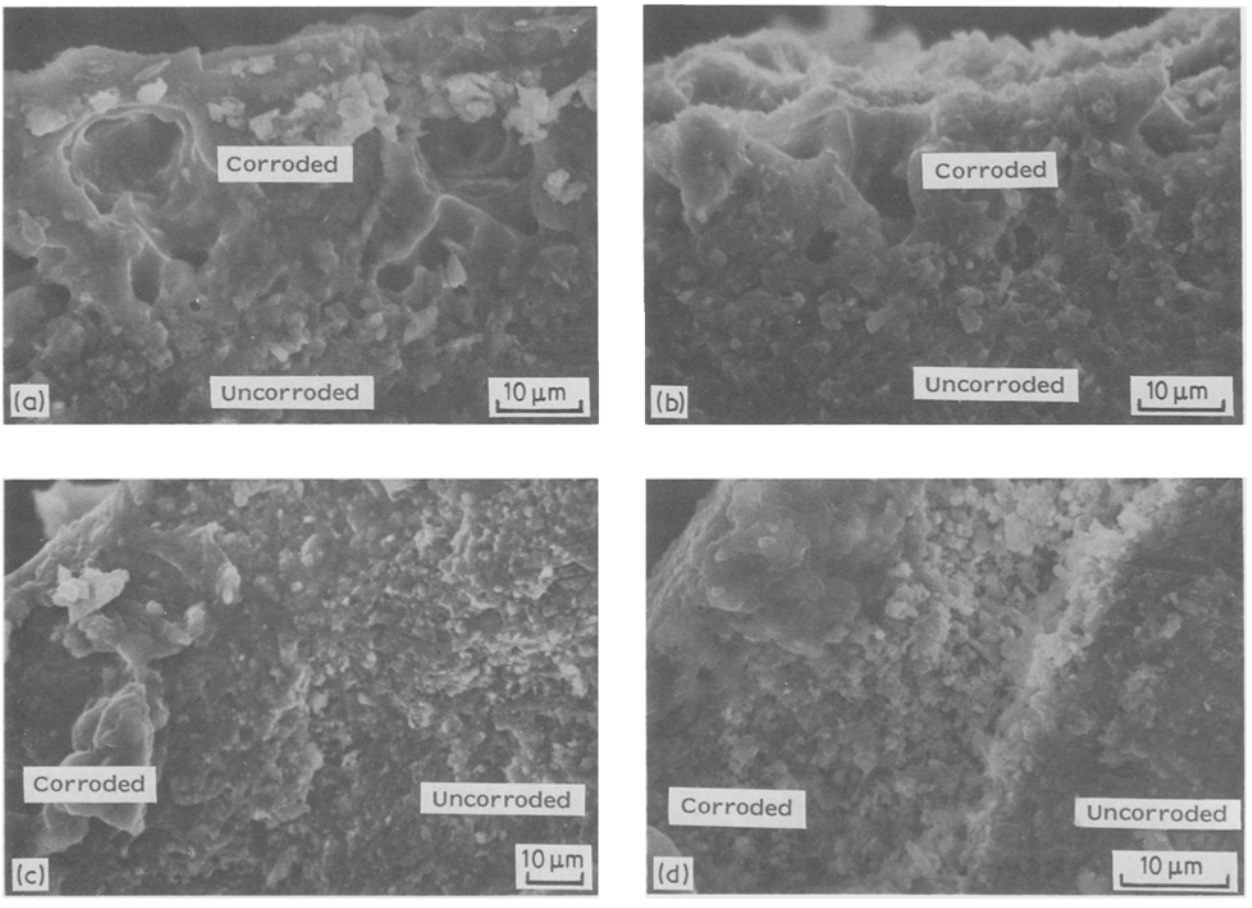

Figure 8 Scanning electron micrographs of the cross-sections of SiAlON-60 immersed (a, b) in K_2SO_4 melts at 1150° C and (c, d) in K_2CO_3 at 925° C for (a, c) 1 h and (b, d) 3 h.

TABLE IV The time prediction of rupture for various Si_3N_4-based ceramics of 50 mm × 50 mm × 50 mm in K_2SO_4 and K_2CO_3 melts at 1100° C

Sample	In K_2SO_4	In K_2CO_3
HIP-Si_3N_4	273 hr	1.47 hr
HP-Si_3N_4	729	27.1
SiAlON-0	1991	29.1
SiAlON-30	616	25.8
SiAlON-60	1765	25.5
SiAlON-100	2127	61.3

with increasing contents of aluminium and yttrium ions in the specimen.

4. The corrosion resulted in a roughness on the surface of the specimens, and degraded the fracture strength to 2/3 to 2/5 of the original values up to a 2% weight loss, and then remained almost constant up to 30% weight loss.

Acknowledgement

This work was supported in part by a grant-in-aid for Energy Research of the Ministry of Education.

References

1. M. I. MAYER and F. L. RILEY, *J. Mater. Sci.* **13** (1978) 1319.
2. E. ERDOES and H. ALTORFER, "Materials and Coatings to Resist High Temperature Corrosion", edited by D. R. Holmes and A. Rahemel (Applied Science, London, 1977) p. 161.
3. R. E. TRESSLER, M. D. MEYSER and T. YONUSHONIS, *J. Amer. Ceram. Soc.* **59** (1976) 278.
4. W. C. BOURNE and R. E. TRESSLER, *Amer. Ceram. Soc. Bull.* **59** (1980) 443.
5. M. K. FERBER and V. J. TENNERY, *ibid.* **62** (1983) 236.
6. P. F. BECHER, *J. Mater. Sci.* **19** (1984) 2805.
7. T. SATO, Y. KANNO, T. ENDO and M. SHIMADA, *Adv. Ceram. Mater.* **2** (1987) 228.
8. J. L. SMIALEK and N. S. JACOBSON, *J. Amer. Ceram. Soc.* **69** (1986) 741.
9. C. P. GAZZARA and D. R. MEISSIER, *Amer. Ceram. Soc. Bull.* **56** (1977) 777.
10. T. SATO, Y. KANNO and M. SHIMADA, *Int. J. High Technol. Ceram.* **2** (1986) 279.

Received 8 June
accepted 20 August 1987